DE GRUYTER OPEN

Journal of ELECTRICAL ENGINEERING, VOL 68 (2017), NO6, 455–462

Convolution implementation with a novel approach of DGHM multiwavelet image transform

Ondrej Kovac*, Jan Mihalik, Iveta Gladisova****

The purpose of this paper is to develop convolution implementation of DGHM (Donovan, Geronimo, Harding, Massopust) multiwavelet image transform using a new approach of ordering wavelet coefficients at the second and higher levels. Firstly, the method of implementation of one-dimensional discrete multiwavelet transform (1D DMWT) for DGHM multiwavelet using discrete convolution and scalar filters is presented. Then, convolution implementation of DGHM multiwavelet image transform by application of 1D DMWT for two dimensions (2D) in a separable way is proposed. Next, the second level of 2D DMWT is performed in three possible ways. The novelty of the proposed implementation is in reordering of L subband wavelet coefficients at the first level into one subimage. The results are evaluated as the energy ratios between the transformed images in L subband at the second level and the input original image. According to the experimental results, the developed implementation of 2D DMWT is approximately 5 % more effective in energy compression than the ones most commonly mentioned in the literature. This paper shows a possibility of convolution implementation of 2D DMWT with higher energy compression.

K e y w o r d s: multiwavelet transform, convolution, prefilter, postfilter, multifilter, compression

1 Introduction

Wavelet transform became popular in the last decades in the field of image compression [1–5]. Multiwavelets offer better properties and results for applications of image compression compared to scalar wavelets [6–8], which can be considered as generalization of scalar wavelets. Multiwavelet transform can have r scale functions and r wavelet functions, so we can say it has multiplicity of r. Most of the developed multiwavelet transforms use two scale functions and two wavelet functions, but theoretically r can reach an optional value [9]. Properties such as orthogonality, symmetry, high order of approximation and short support are the basis for the successful application of multiwavelets in image compression [10–12]. Such properties cannot be achieved by scalar wavelets. Well known multiwavelets are DGHM (Donovan, Geronimo, Harding, Massopust), also CL(0,2) and CL(0,3) [13, 14].

The second chapter of the present paper gives convolution implementation of 1D DMWT with DGHM multiwavelets. In this chapter, the input signal preprocessing is presented with the analysis of convolution properties between pulse responses of scalar filters and extended input [15]. The third chapter is focused on convolution implementation of 2D DMWT of images for DGHM multiwavelets. 2D DMWT is achieved by application of 1D DMWT at first on rows and consequently after the transform on columns [16, 17]. Also, analysis of the second level of 2D DMWT is given. There are three options presented for the second level of transform. Two of these options are well known and the third was proposed by us. In chapter four, the results of 2D DMWT of images for the first and the second levels are presented. The analysis is done on seven input images. The results are evaluated as energy ratios between energy of L subbands of the

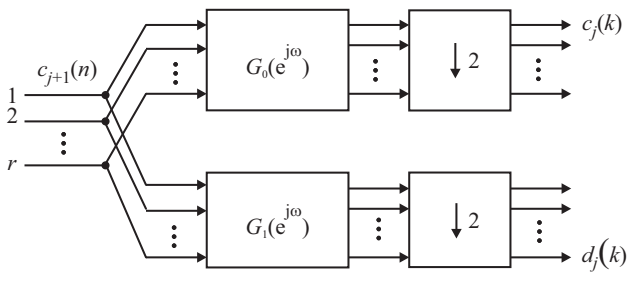

Fig. 1. Implementation of the forward and backward 1D DMWT for j-level

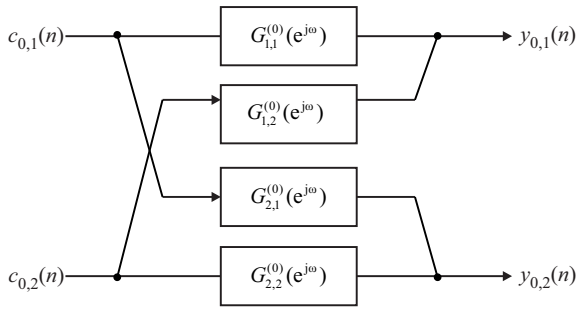

Fig. 2. LP multi-filter for $r = 2$ is composed of scalar filters

* Department of Technologies in Electronics, ** Department of Electronics and Multimedia Communications, Faculty of Electrical Engineering and Informatics, Technical University of Košice, Slovakia, ondrej.kovac@tuke.sk, jan.mihalik@tuke.sk, iveta.gladisova@tuke.sk

DOI: 10.1515/jee-2017–0080, Print (till 2015) ISSN 1335-3632, On-line ISSN 1339-309X

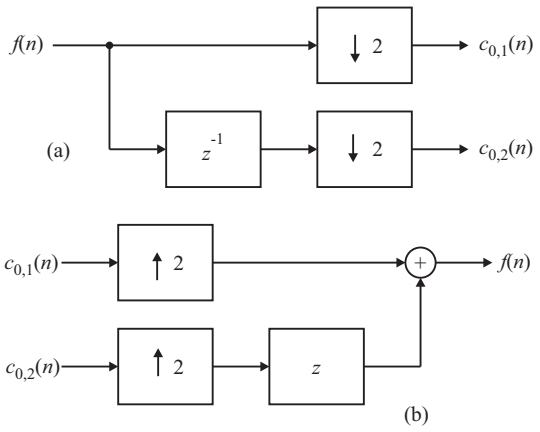

Fig. 3. Filters for 1D DMWT with DGHM multiwavelets: (a) – pre-filter, and (b) – post-filter

transformed images and the input images. The conclusion summarizes the achieved results.

2 Convolution implementation of 1D DMWT with DGHM multiwavelets

Implementation of the forward 1D DMWT using banks of multi (vector) filters and also multi decimators and interpolators for j-level [18, 19] is given in Fig. 1.

Each multi-filter for one level of the forward and backward 1D DMWT with $r = 2$ has two inputs and two outputs, as shown in Fig. 1. For example, low pass multi-filter (LP) with matrix frequency response

$$\mathbf{G}_0(e^{j\omega}) = \left[G^{(0)}_{l,m}(e^{j\omega})\right]\big|_{2\times 2}, \quad r, l, m = 2$$

is composed of scalar filters with frequency responses $G^{(0)}_{1,1}(e^{j\omega})$ as shows Fig. 2, where $y_{0,1}(n)$ and $y_{0,2}(n)$ are samples of sub-channels on outputs of this multi-filter. Analogously, it is possible to express high pass multi-filter (HP) by matrix frequency response $\mathbf{G}_1(e^{j\omega})$ as well as with two inputs and outputs.

One of the best known 1D DMWT with multiplicity $r = 2$ is designed using Donovan, Geronimo, Harding and Massopust multiwavelets [13]. Matrix samples of pulse responses $\mathbf{G}_0(k)$ and $\mathbf{G}_1(k)$ as 2×2 matrices are shown below

$$\begin{aligned} \mathbf{G}_0(0) &= \begin{bmatrix} \frac{3}{10} & \frac{2\sqrt{2}}{5} \\ -\frac{\sqrt{2}}{40} & -\frac{3}{20} \end{bmatrix}, \quad \mathbf{G}_0(1) = \begin{bmatrix} \frac{3}{10} & 0 \\ \frac{9\sqrt{2}}{40} & \frac{1}{2} \end{bmatrix} \\ \mathbf{G}_0(2) &= \begin{bmatrix} 0 & 0 \\ \frac{9\sqrt{2}}{40} & -\frac{3}{20} \end{bmatrix}, \quad \mathbf{G}_0(3) = \begin{bmatrix} 0 & 0 \\ -\frac{\sqrt{2}}{40} & 0 \end{bmatrix} \end{aligned} \tag{1}$$

$$\begin{aligned} \mathbf{G}_1(0) &= \begin{bmatrix} -\frac{\sqrt{2}}{40} & -\frac{3}{20} \\ -\frac{1}{20} & -\frac{3\sqrt{2}}{20} \end{bmatrix}, \quad \mathbf{G}_1(1) = \begin{bmatrix} \frac{9\sqrt{2}}{40} & -\frac{1}{2} \\ \frac{9}{20} & 0 \end{bmatrix} \\ \mathbf{G}_1(2) &= \begin{bmatrix} \frac{9\sqrt{2}}{40} & -\frac{3}{20} \\ -\frac{9}{20} & \frac{3\sqrt{2}}{20} \end{bmatrix}, \quad \mathbf{G}_1(3) = \begin{bmatrix} -\frac{\sqrt{2}}{40} & 0 \\ -\frac{1}{20} & 0 \end{bmatrix} \end{aligned} \tag{2}$$

Contrary to classical 1D DWT, the input scalar discrete signal has to be transformed to the vector form before making forward 1D DMWT and has to be restored from the vector form after performing backward 1D DMWT. These two operations are known as pre-filtering and post-filtering [20, 21].

Figure 3(a) shows the division of the input scalar signal $f(n)$ into sequences of even and odd samples, *ie*

$$\begin{bmatrix} c_{0,1}(n) \\ c_{0,2}(n) \end{bmatrix} = \begin{bmatrix} f(2n) \\ f(2n+1) \end{bmatrix}. \tag{3}$$

The post-filtering as an inverse process compared to pre-filtering is shown in Fig. 3(b). The sequences of even and odd samples will merge into one sequence $f(n)$.

Table 1. Pulse responses with properties of scalar filters for LP multi-filter

Scalar filter	Length	Symmetry
$G^0_1 = G^{(0)}_{1,1} \to g^0_1 = \left\{\frac{3}{10}, \frac{3}{10}\right\}$	Even	Even
$G^0_2 = G^{(0)}_{1,2} \to g^0_2 = \left\{\frac{2\sqrt{2}}{5}\right\}$	Odd	Even
$G^0_3 = G^{(0)}_{2,1} \to g^0_3 = \left\{-\frac{\sqrt{2}}{40}, \frac{9\sqrt{2}}{40}, \frac{9\sqrt{2}}{40}, -\frac{\sqrt{2}}{40}\right\}$	Even	Odd
$G^0_4 = G^{(0)}_{2,2} \to g^0_4 = \left\{-\frac{3}{20}, \frac{1}{2}, -\frac{3}{20}\right\}$	Odd	Odd

Table 2. Pulse responses with properties of scalar filters for HP multi-filter

Scalar filter	Length	Symmetry
$G^1_1 = G^{(1)}_{1,1} \to g^1_1 = \left\{-\frac{\sqrt{2}}{40}, \frac{9\sqrt{2}}{40}, \frac{9\sqrt{2}}{40}, -\frac{\sqrt{2}}{40},\right\}$	Even	Even
$G^1_2 = G^{(1)}_{1,2} \to g^1_2 = \left\{-\frac{3}{20}, -\frac{1}{2}, -\frac{3}{20}\right\}$	Odd	Even
$G^1_3 = G^{(1)}_{2,1} \to g^1_3 = \left\{-\frac{1}{20}, \frac{9}{20}, -\frac{9}{20}, \frac{1}{20}\right\}$	Even	Odd
$G^1_4 = G^{(1)}_{2,2} \to g^1_4 = \left\{-\frac{3\sqrt{2}}{20}, 0, \frac{3\sqrt{2}}{20}\right\}$	Odd	Odd

Table 3. The properties of convolution depending on the extension and the filters properties

Mode	Signal extension	Filter		Properties of convolution
		Symmetry	Length	
1	Even whole-sample	Even	Odd	Even whole-sample
2	Even half-sample	Even	Even	Even whole-sample
3	Even whole-sample	Odd	Odd	Odd whole-sample
4	Even half-sample	Odd	Even	Odd whole-sample

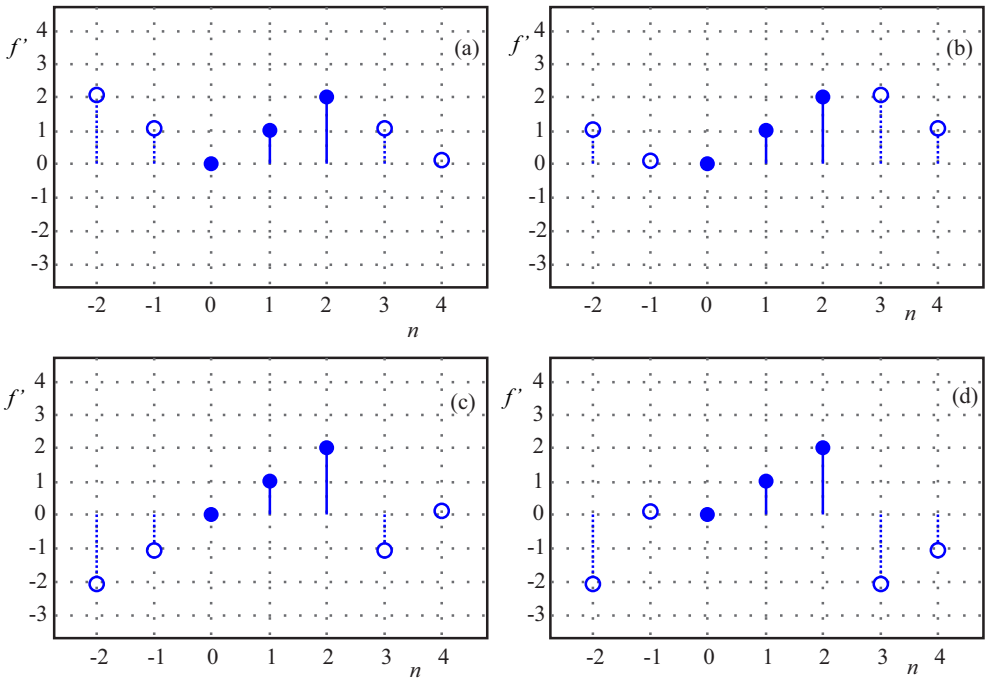

Fig. 4. The both kinds of extensions WSS: (a) – even, (c) – odd, HSS: (b) – even, (d) – odd

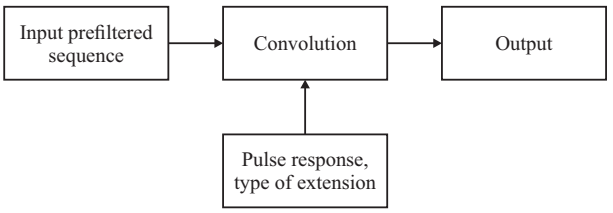

Fig. 5. The basic idea of convolution implementation of 1D DMWT

Based on matrix samples $\mathbf{G}_0(k)$, $\mathbf{G}_1(k)$ from (1) and (2) pulse responses for LP and HP multi-filters can be expressed. Frequency responses of their scalar filters and the corresponding pulse responses with properties such as length and symmetry are in Tables 1 and 2.

2.1 Input Signal Preprocessing

As signals $c_{0,1}(n)$, $c_{0,2}(n)$ of the pre-filter are of finite length, there is a possibility of unwanted border distortion of the calculated convolution with appropriate pulse responses of the scalar filters. To eliminate this distortion, the signals $c_{0,1}(n)$, $c_{0,2}(n)$ are extended by two kinds of symmetrical extensions. The first one is a whole sample symmetric (WSS) extension and the second one is a half sample symmetric (HSS) extension [7, 22]. Figure 4 shows the input signal $f(n)$ (peaks ended by dark spot) and its possible extensions $f'(n)$.

Table 3 shows clearly that there are two possible ways of extension – even half-sample and even whole-sample. As input sequences are extended, it is possible to cut off the extension after convolution without any border distortion. So, the output sequence has the same length as the input sequence before the extension. It is possible to say that the convolution result has always properties of whole-sample symmetry independently of the extension of the input signal. The basic idea of convolution implementation of 1D DMWT is given in Fig. 5.

In general, both kinds of extensions can be used, but for our convolution implementation of 1D DMWT with DGHM multiwavelets, the WSS method is used. Possible extensions and properties of convolution for the different combinations of symmetry and length of pulse responses of the scalar filters for multi-filters are listed in Tab. 3.

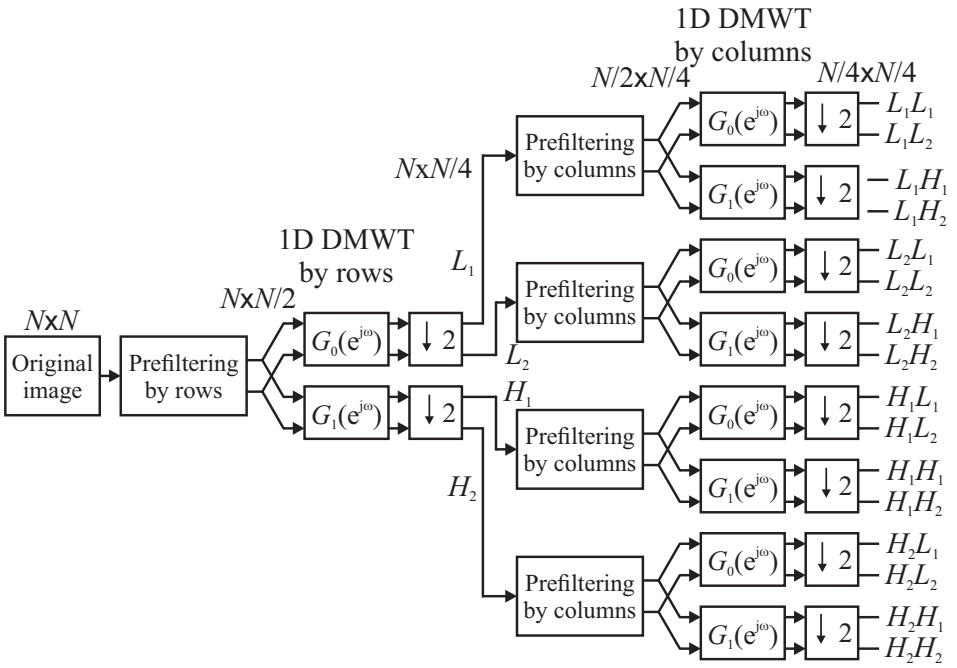

Fig. 6. The architecture for the first level of 2D DMWT

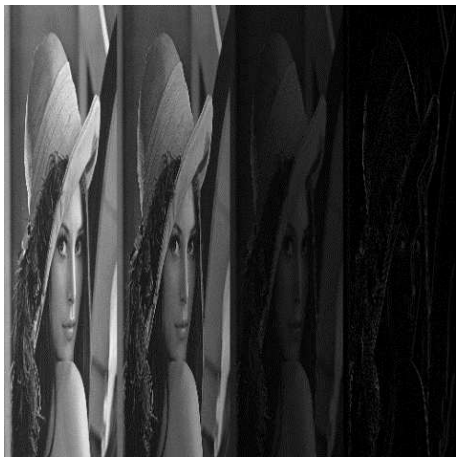

Fig. 7. The result of 1D DMWT by rows

L_1L_1	L_1L_2	L_1H_1	L_1H_2
L_2L_1	L_2L_2	L_2H_1	L_2H_2
H_1L_1	H_1L_2	H_1H_1	H_1H_2
H_2L_1	H_2L_2	H_2H_1	H_2H_2

Fig. 8. The arrangement of sub-images at the first level of 2D DMWT

The input pre-filtered sequence $c_{0,1}(n)$ or $c_{0,2}(n)$ for the specific type of scalar filter is extended according to Tab. 3. For LP multi-filter and its corresponding scalar filters outputs $y_{0,1}(k)$ and $y_{0,2}(k)$ are calculated by

$$y_{0,1}(k) = \sum_n g_1^{(0)}(k-n)c_{0,1}(n) + \sum_n g_2^{(0)}(k-n)c_{0,2}(n)\,, \quad (4)$$

$$y_{0,2}(k) = \sum_n g_3^{(0)}(k-n)c_{0,1}(n) + \sum_n g_4^{(0)}(k-n)c_{0,2}(n)\,. \quad (5)$$

The length of these signals has to be adjusted to the length of input signals of LP multi-filter before their extensions. Outputs $y_{1,1}(k)$ and $y_{1,2}(k)$ of HP multi-filters with subsequent determination of their length are calculated analogically. Finally, the outputs of LP and HP multi-filters are decimated by decimation factor 2, resulting in the first level scale $c_{-1}(k) = [c_{-1,1}(k), c_{-1,2}(k)]^\top$ and detail $d_{-1}(k) = [d_{-1,1}(k), d_{-1,2}(k)]^\top$ coefficients of the forward 1D DMWT with DGHM.

3 Convolution implementation of 2D DMWT of images

1D DMWT implemented in Chapter 2 can be easily applied on 2D DMWT on the basis of core separation [9]. Figure 7 shows the architecture of 2D DMWT where in the input there is an original image of size $N \times N$ pixels, which is pre-filtered by all its rows according to Fig. 3.

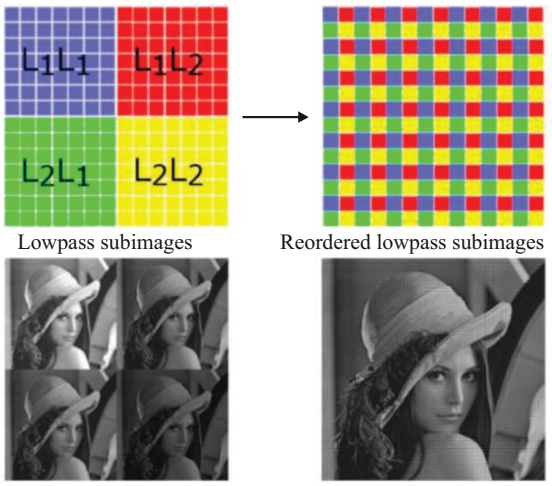

Fig. 9. The reordering of wavelet coefficients of subimages L_1L_1, L_1L_2, L_2L_1 and L_2L_2 into one reordered lowpass sub-image

After pre-filtering we have two sub-images of the size $N \times (N/2)$ pixels. As a result of further application of 1D DMWT for rows of subimages we have four subimages of wavelets coefficients L_1, L_2, H_1 and H_2 of the size $N \times (N/4)$ pixels on the outputs of decimators (Fig. 7).

The presented prefiltering and 1D DMWT is then applied for columns of subimages of wavelet coefficients L_1, L_2, H_1 and H_2 as shown in Fig. 7. This results in 16 subimages of wavelet coefficients L_1L_1, L_1L_2, L_1H_1, L_1H_2, L_2L_1, L_2L_2, L_2H_1, L_2H_2, H_1L_1, H_1L_2, H_1H_1, H_1H_2, H_2L_1, H_2L_2, H_2H_1 and H_2H_2 at the first level of 2D DMWT that are shown in Fig. 8.

3.1 The Second Level of 2D DMWT

Calculation for the second level of image transform by 2D DMWT is analogical to transform at the first level [14, 23]. But there are three possible options for input of the second level of 2D DMWT. In the first option (Option 1), the input L subband consisting of subimages L_1L_1, L_1L_2, L_2L_1 and L_2L_2 is considered. These subimages are transformed together. In this case, the results are 16 subimages for the second level of 2D DMWT and also 12 subimages from the first level. In the second option (Option 2), the subimages of the L subband are transformed independently from each other. The results obtained are 64 subimages of wavelet coefficients (16 for each L subimage from the first level and 12 subimages of details from the first level). The third option (Option 3) at the second level of 2D DMWT, designed by us, is based on the reordering of wavelet coefficients of subimages L_1L_1, L_1L_2, L_2L_1 and L_2L_2 (Fig. 9, on the left) into one reordered lowpass subimage (Fig. 9, on the right). After transform of this reordered lowpass subimage we get 16 subimages at the second level and from the first level we have 12 subimages. The third, fourth *etc* level of 2D DMWT can be calculated in the same manner, while each next level of 2D DMWT can be achieved by transform of subimages ${}^{K}L_iL_j$, where $K = 2, 3, 4, \ldots$ and $i, j = 1, 2$.

4 Experimental results

Based on the given theory, the convolution implementation of 2D DMWT was done. For illustration, Fig. 10(a) gives subimages of 2D DMWT of image Lena of the size 512×512 pixels at the first level. Figure 10(b) shows the result of 2D DMWT at the second level using Option 1. Figure 10(c) shows the transform result at the second level using Option 2. The transform result at the second level using Option 3 is shown in Fig. 10(d).

Figure 11 shows a normalized energy distribution of the transformed image of Lena. The distribution at the first level is shown in Fig. 11(a). Energy distribution for 2D DMWT at the second level achieved by Options 1, 2 and 3 is shown in Fig. 11(b),(c),(d), respectively. For better presentation, the energies are normalized by a maximum value of the transformed images.

From Fig. 10(a) and Fig. 11(a) it is obvious that subimages L_1L_1, L_1L_2, L_2L_1 and L_2L_2 are highly correlated and have high energy (they represent low-pass subband). Otherwise, all other subimages at the first level L_1H_1, L_1H_2, L_2H_1, L_2H_2, H_1L_1, H_1L_2, H_1H_1, H_1H_2, H_2L_1, H_2L_2, H_2H_1, H_2H_2 are uncorrelated and have low energy (they represent high-pass subband). Analogically, this is also true for subimages at the second level of 2D DMWT. Subimages ${}^{2}L_1L_1$, ${}^{2}L_1L_2$, ${}^{2}L_2L_1$, ${}^{2}L_2L_2$ remain correlated and have high energy. All other

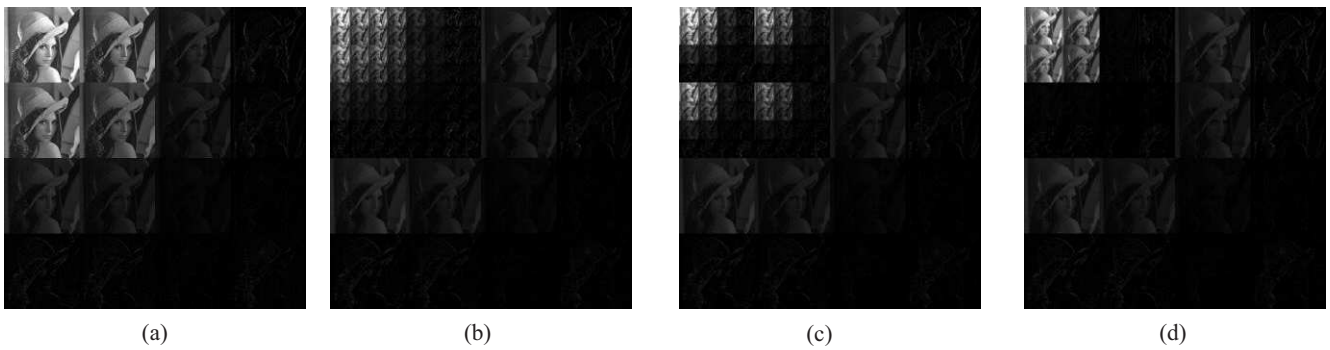

Fig. 10. The subimages of 2D DMWT of image Lena of the size 512×512 pixels: (a) – at the first level and sub-images at the second level of 2D DMWT for: (b) – Option 1, (c) – Option 2, and (d) – Option 3

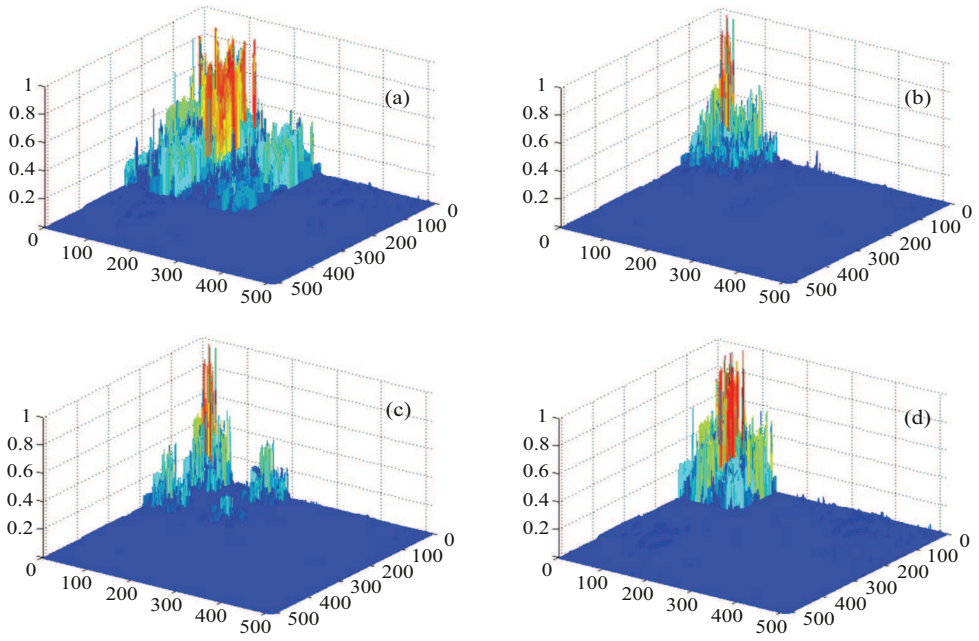

Fig. 11. A normalized energy distribution of 2D DMWT of the Lena image: (a) – at the first level and at the second level for (b) – Option 1, (c) – Option 2, (d) – Option 3

Table 4. The alignment of the energy ratios in % into the subimages at the first level of 2D DMWT

	L_1	L_2	H_1	H_2
L_1	45.9	19.93	1.86	0.25
L_2	19.88	8.68	0.81	0.15
H_1	1.86	0.81	0.08	0.02
H_2	0.16	0.11	0.02	0.07

subimages 2D DMWT at the second level ${}^2L_1H_1$, ${}^2L_1H_2$, ${}^2L_2H_1$, ${}^2L_2H_2$, ${}^2H_1L_1$, ${}^2H_1L_2$, ${}^2H_1H_1$, ${}^2H_1H_2$, ${}^2H_2L_1$, ${}^2H_2L_2$, ${}^2H_2H_1$, ${}^2H_2H_2$ are uncorrelated with low energy. Energy is calculated as a sum of quadratic values of wavelets coefficients. Ratios (in %) of the energy of separate wavelet subimages to the energy of the input Lena image for the first level 2D DMWT are listed in Tab. 4.

From Tab. 4 it is obvious that at the first level of 2D DMWT the ratio of energies of the lowpass quadrant L (represented by subimages L_1L_1, L_1L_2, L_2L_1 and L_2L_2) to the total energy is 94.39 %. The rest 5.61 % of the energy ratio is divided between twelve subimages L_1H_1, L_1H_2, L_2H_1, L_2H_2, H_1L_1, H_1L_2, H_1H_1, H_1H_2, H_2L_1, H_2L_2, H_2H_1 and H_2H_2, which represent the highpass quadrants. From the data given above, it can

Table 5. The resultant energy ratios (in %) at the first and second level for Options 1, 2 and 3 of 2D DMWT

Input image	Energy ratio between L subband of the first level and input image	Energy ratio between L subband of the second level and input image			Difference between ratios		
		Option 1	Option 2	Option 3	Option1 & Option 2	Option1 & Option 3	Option2 & Option 3
Baboon	93.5	87.05	87.23	92.37	0.18	5.32	5.14
Forrest	94.5	87.06	87.72	93.78	0.66	6.73	6.06
Apache	94.5	88.74	88.88	93.99	0.14	5.26	5.12
Castle	94.5	88.75	88.81	93.79	0.06	5.05	4.99
Lena	94.4	88.19	88.33	93.58	0.14	5.39	5.25
Missouri	94.5	88.97	89.03	94.01	0.06	5.04	4.98
Elephant	94.5	88.62	88.75	93.78	0.13	5.16	5.03
Dog	94.6	89.07	89.26	94.20	0.19	5.13	4.94
Average	94.4	88.32	88.50	93.69	0.19	5.38	5.19
Deviation	0.33	0.76	0.65	0.53	0.18	0.52	0.34

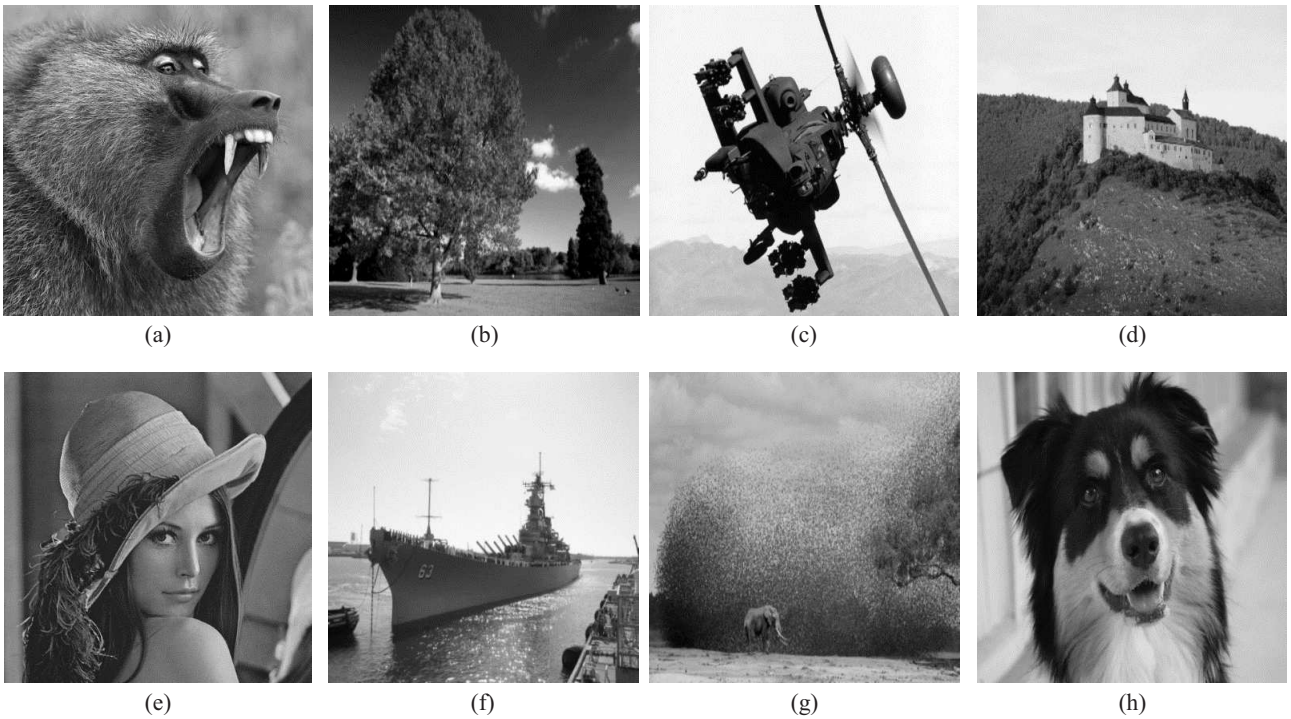

(a) (b) (c) (d)

(e) (f) (g) (h)

Fig. 12. Input images: (a) – Baboon, (b) – Forrest, (c) – Apache, (d) – Castle, (e) – Lena, (f) – Missouri, (g) – Elephant, (h) – Dog

be stated that by 2D DMWT energy compression of image is achieved. The ratio for the second level of 2D DMWT in lowpass subimages is 88.188 % (in case of Option 1) and 88.331 % (in case of Option 2). Maximum energy ratio 93.579 % is achieved by reordered lowpass subimages (Option 3). From the above and from Fig. 10 and Fig. 11 we can see that a better degree of energy compression at the second level of 2D DMWT is achieved by transform of the L subimages reordered into one subimage. The experiment described above was performed with other seven input images in Fig. 12. In Tab. 5 the energy ratios at the second level of 2D DMWT for each image are listed.

From Tab. 5 it is apparent that the energy ratios of well-known methods represented by Option 1 and 2 are similar. The average value for Option 1 is 88.306 % and for Option 2 it is 88.502 %. Energy ratio of all of the input images does not exceeded 90 %. The average value of differences between Option 1 and 2 is only 0.196 % with deviation 0.182 %. On the other hand, the average value of energy ratios for Option 3 is 93.69 % with deviation 0.529 %. Our proposed convolution implementation of 2D DMWT with a novel approach at the second level achieves higher energy ratio of L subband for each of the input images. Also, it can be seen that most of the image energy at the second level is compressed into L subband and in the other subbands there remains only low energy. The average value of the increase of the energy ratio of L subband for Option 3 compared to the energy ratio of the L subband for Option 2 is 5.188 % with deviation 0.345 % and 5.384 % for Option 1 with deviation 0.521 %.

6 Conclusion

Application of 1D DMWT to multiwavelet image transform is a generally known approach. The input signal is divided into even and odd sequences by using prefilters and after that the convolution between the pulse responses of four scalar filters of lowpass and highpass multi-filters and symmetrically extended sequences is used in 1D DMWT. 1D DMWT can be easily applied to 2D DMWT on the basis of the core separation. One of the goals of this paper is to analyse energy compression. The energy ratio is calculated and evaluated as ratio energy of L subimages to the energy of the input image. DMWT energy is compressed into a zone of low frequencies - into L subbands that is the same as in other orthogonal transforms. The main purpose of this paper is convolution implementation with a novel approach at the second and higher levels of 2D DMWT of images. From theory it is known that the inputs of the second level of 2D DMWT are wavelet coefficients from the first level. For the transform at the second level, however, there arises a question, which of the subbands are supposed to be the input to the processor 2D DMWT at the second level. There are only two ways mentioned in the literature. The first one is based on the transform of all subimages of L subband together. In the paper, this method is called as Option 1. The advantage of this approach is that there is no need of subbands reordering. However, from the point of view of energy compression ratio this method is the worst. The second approach (Option 2) is that the inputs of the second level are all L subimages transformed one by one. In this way, a little higher energy ratio is achieved, but the disadvantage is creation of 64 subimages at the second level of 2D DMWT. The proposed convolution imple-

mentation with a novel approach (Option 3) is that the input is indeed all L subimages, but before the transform itself, the wavelet coefficients are reordered into one L subimage. Using this approach, a higher energy ratio is achieved compared to the ones of transform of non-reordered L subimages. We demonstrated this approach on the set of input images and achieved an average of 5.2 % enhancement of the energy ratio for all of them shown in this paper. Experimental results demonstrated that the proposed technique provided sufficient higher energy compression ratios compared to other traditional techniques, which enables to achieve higher data compression of the image coding systems using 2D DMWT.

References

[1] K. Rajakumar and T. Arivoli, "Implementation of Multiwavelet Transform Coding for Lossless Image Compression", *Proc. of International Conference on Information Communication and Embedded Systems (ICICES)*, Chennai, 2013, pp. 634–637.

[2] K. Bao and X. G. Xia, "Image Compression Using a New Discrete Multiwavelet Transform and a New Embedded Vector Quantization", *IEEE Trans. on Circuits and Systems for Video Technology*, vol. 10, no. 6, 2000, pp. 833–842.

[3] N. Sriraam and R. Shyamsunder, "3-D Medical Image Compression Using 3-D Wavelet Coders", *Digital Signal Processing*, vol. 21, no. 1, 2011, pp. 100–109.

[4] J. Mihalík, J. Zavacký and J. Dzivý, "Perfect Reconstruction 2DQMF Bank for Subband Image Coding", *Journal of Electrical Engineering*, vol. 47, no. 7-8, 1996, pp. 195–201.

[5] O. Kováč and J. Mihalík, "Lossless Encoding of 3D Human Head Model Textures", *Acta Electrotechnica et Informatica*, vol. 15, no. 3, 2015, pp. 18–23.

[6] B. E. Usevitch, "A Tutorial on Modern Lossy Wavelet Image Compression: Foundations of JPEG 2000", *IEEE Signal Processing Mag.*, vol. 18, no. 5, 2001, pp. 22–35.

[7] M. B. Martin and A. E. Bell, "New Image Compression Techniques Using Multiwavelets and Multiwavelet Packets", *IEEE Trans. on Image Processing*, vol. 10, no. 4, 2001, pp. 500–510.

[8] W. Kim and Ch. Li, "On Preconditioning Multiwavelet System for Image Compression", *International Journal of Wavelets, Multiresolution and Information Processing*, vol. 1, no. 1, 2003, pp. 51–74.

[9] F. Keinert, "", *Wavelets and Multiwavelets*, Champan & Hall/ CRC, 2004.

[10] C. K. Chui and J. A. Lian, "A Study of Orthonormal Multi wavelets", *Applied Numerical Mathematics*, vol. 20, no. 3, 1996, pp. 273–298.

[11] T. Ch. Hsung, D. P. Lun, Y. Shum and K. C. Ho, "Generalized Discrete Multiwavelet Transform with Embedded Orthogonal Symmetric Prefilter Bank", *IEEE Transactions on Signal Processing*, vol. 55, no. 12, 2007, pp. 5619–5629.

[12] R. Kusum and R. Sharma, "Study of Image Fusion Using Discrete Wavelet and Multiwavelet Transform", *International Journal of Innovative Research Computer and Communication Engineering*, vol. 1, no. 4, 2013, pp. 95–99.

[13] G. C. Donovan, J. S. Geronimo, D. P. Harding and P. R. Massopust, "Connstruction of Orthogonal Wavelets Using Fraction Interpolation Functions", *SIAM Journal on Mathematical Analysis*, vol. 27, no. 4, 1996, pp. 1158–1192.

[14] L. Wei, "An Image Coding Method Based on Multi Wavelet Transform", *4th International Conference on Image and Signal Processing*, vol. 2, 2011, pp. 607–610.

[15] V. Strela, P. Heller, G. Strang, P. Topiwala and C. Heil, "The Application of Multiwavelet Filter Banks to Signal and Image Processing", *IEEE Trans. Image Processing*, vol. 8, no. 4, 1999, pp. 548–563.

[16] T. S. Anand, K. Narasimhan and P. Saravanan, "Performance Evaluation of Image Fusion Using the Multi Wavelet and Curvelet Transforms", *IEEE International Conference on Advances Engineering*, Science and Management (ICAESM), 2012, pp. 121–129.

[17] D. Dia *et al*, "Multi-level Discrete Wavelet Transform Architecture Design", *Proceedings of the World Congress on Engineering*, WCE 2009, vol. I., London, U.K., 2009, pp. 1–2.

[18] J. Y. Tham, L. X. Shen, S. L. Lee and H. H. Tan, "A General Approach for Analysis and Application of Discrete Multiwavelet Transforms", *IEEE Trans. on Signal Processing*, vol. 48, no. 2, 2000, pp. 457–464.

[19] I. Ram, M. Elad and I. Cohen, "Generalized Tree Based Wavelet Transform", *IEEE Transactions on Signal Processing*, vol. 59, no. 9, 2011, pp. 4199–4210.

[20] D. P. Hardin and D. W. Roach, "Multi-Wavelet Prefilters part I :Orthogonal Prefilters Pre serving Approximation Order", *IEEE Transactions on Circuits and Systems II*, vol. 45, 1998, pp. 1106–1112.

[21] K. Hardin, D. P. Attakitmongcol and D. M. Wilkes, "Multiwavelet Prefilters – part II: Optimal Orthogonal Prefilters", *IEEE Trans. on Image Processing*, vol. 10, 2001, pp. 1476–1487.

[22] G. Iovane and P. Giordano, "Wavelets and Multiresolution Analysis: Nature of $\varepsilon^{(\infty)}$ Cantorian Space Time", *Chaos Solitons & Fractals*, vol. 32, 2007, pp. 896–910.

[23] A. Fathi and A. R. N. Nilchi, "Efficient Image Denoising Method Based on a New Adaptive Wavelet Packet Thresholding Function", *IEEE Transaction of Image Processing*, vol. 21, no. 9, 2012, pp. 3981–3990.

Received 31 January 2017

Ondrej Kováč was born on 1986 in Košice. In 2011 he received the Ing degree in Multimedia telecommunications from the Faculty of Electrical Engineering, Technical University of Košice. His PhD thesis topic was focused to texture generating, 3D modeling and coding of human head. Since June 2015, he has been working as assistant professor at the Department of Technologies in Electronics, Technical University of Košice.

Ján Mihalík graduated from the Technical University of Bratislava in 1976. In 1979, he joined the Faculty of Electrical Engineering and Informatics of Technical University at Košice, where he received his PhD degree of radioelectronics in 1985. Currently, he is a full professor of electronics and telecommunications and the head of the Laboratory of Digital Image Processing and Video-communications at the Department of Electronics and Multimedia Telecommunications. His research interests include information theory, image and video coding, digital image and video processing and multimedia video-communications.

Iveta Gladišová graduated from the Technical University of Košice in 1984. She is employed at same university of Košice, where received her PhD Degree in Radioelectronics in 1997. She is Assistant Professor at the Department of Electronics and Multimedia Telecommunications, Faculty of Electrical Engineering and Informatics, Technical University, Košice. Her research interests include entropy coding, segmentation, vector quantization and digital image processing.